Received: 21 March 2020 | Revised: 28 January 2021 | Accepted: 26 February 2021

DOI: 10.1096/fj.202000662RR

RESEARCH ARTICLE

THE FASEB JOURNAL

E-selectin negatively regulates polymorphonuclear neutrophil transmigration through altered endothelial junction integrity

Dandan Huang[1,2] | **Qihan Ding**[1,2] | **Shenbao Chen**[1,2] | **Shouqin Lü**[1,2] | **Yan Zhang**[1,2] | **Mian Long**[1,2,3]

[1]Center for Biomechanics and Bioengineering, Key Laboratory of Microgravity (National Microgravity Laboratory) and Beijing Key Laboratory of Engineered Construction and Mechanobiology, Institute of Mechanics, Chinese Academy of Sciences, Beijing, China

[2]School of Engineering Science, University of Chinese Academy of Sciences, Beijing, China

[3]Lead Contact, Beijing, China

Correspondence
Yan Zhang and Mian Long, Center for Biomechanics and Bioengineering, Key Laboratory of Microgravity (National Microgravity Laboratory) and Beijing Key Laboratory of Engineered Construction and Mechanobiology, Institute of Mechanics, Chinese Academy of Sciences, Beijing 100190, China.
Email: zhangyan@imech.ac.cn (Y. Z.); mlong@imech.ac.cn (M. L.)

Funding information
National Natural Science Foundation of China (NSFC), Grant/Award Number: 31627804, 91642203, 11772345 and 91539119; National Key Rsearch and Development Program of China, Grant/Award Number: 2016YFA0501601; Chinese Academy of Sciences Strategic Priority Research Program, Grant/Award Number: XDB22040101; Frontier Science Key Project, Grant/Award Number: QYZDJ-SSW-JSC018

Abstract

Transendothelial migration (TEM) of neutrophils under blood flow is critical in the inflammatory cascade. However, the role of endothelial plasticity in this process is not fully understood. Therefore, we used an in vitro model to test the dynamics of human polymorphonuclear neutrophil (PMN) TEM across lipopolysaccharide-treated human umbilical vein endothelial cell (HUVEC) monolayers. Interestingly, shRNA-E-selectin knockdown in HUVECs destabilized endothelial junctional integrity by reducing actin branching and increasing stress fiber at cell–cell junctions. This process is accomplished by downregulating the activation of cortactin and Arp2/3, which in turn alters the adhesive function of VE-cadherin, enhancing PMN transmigration. Meanwhile, redundant P-selectins possess overlapping functions in E-selectin-mediated neutrophil adhesion, and transmigration. These results demonstrate, to our knowledge, for the first time, that E-selectins negatively regulate neutrophil transmigration through alterations in endothelial plasticity. Furthermore, it improves our understanding of the mechanisms underlying actin remodeling, and junctional integrity, in endothelial cells mediating leukocyte TEM.

KEYWORDS

cytoskeletal remodeling, endothelial integrity, E-selectin, neutrophil, transmigration

Abbreviations: Ab, antibody; AFM, atomic force microscope; AJ, adherence junctions; ANOVA, analysis of variance; Arp2/3, actin-related protein 2/3 complex; bFGF, basic fibroblast growth factor; BSA, bovine serum albumin; Ct, the cycle time; DIC, differential interference contrast; DMEM, Dulbecco's modification of Eagle's medium Dulbecco; DMSO, dimethyl sulfoxide; DPBS, Dulbecco's phosphate-buffered saline; EC, endothelial cell; EDTA, ethylenediaminetetraacetic acid; EGTA, ethylene glycol bis (2-aminoethyl ether) tetraacetic acid; Erk, extracellular regulated protein kinases; ESL-1, E-selectin ligand-1; FACS, flowcytometer; FBS, fetal bovine serum; HEPES, 4-(2-hydroxyethyl)-1-piperazineethanesulfonic acid; HUVEC, human umbilical vein endothelial cell; ICAM-1, intercellular cell adhesion molecule; JAIL, junction-associated intermittent lamellipodia; IL-1β, interleukin-1β; LPS, lipopolysaccharide; MAPK, mitogen-activated protein kinases; MEM NEAA, MEM non-essential amino acids; MLC, myosin light chain; NP-40, nonyl phenoxypolyethoxylethanol; PFQNM, Peakforce QNM; PLA, proximity ligation assay; PMN, polymorphonuclear neutrophil; PMSF, Phenylmethanesulfonyl fluoride; PSGL-1, P-selectin glycoprotein ligand-1; PVDF, Polyvinylidene fluoride; QNM, quantitative nanomechanics; qPCR, quantitative real-time PCR; RT, room temperature; scr, the scramble plasmid; SDS-PAGE, sodium dodecyl sulfate-Polyacrylamide gel electrophoresis; SE, standard error of mean; shE-sel, E-selectin shRNA plasmid; shRNA, short hairpin RNA; TEM, transendothelial migration; TNF-α, tumor necrosis factor-α; VCAM-1, vascular cell adhesion molecule; VE-cadherin, vascular endothelial cadherin.

1 | INTRODUCTION

Leukocyte transendothelial migration (TEM) is critical for the defense of exogenous infections and repair of injured tissue. This multistep process is orchestrated by several families of cellular adhesion molecules, including selectins, integrins, and their ligands on the endothelium, which mediate tethering, rolling, firm adhesion, and transmigration of circulating leukocytes.[1] Selectins are known to mediate the initial interactions of leukocytes with endothelial cells (ECs), slowing down the flow of leukocytes, also considered a prerequisite for integrin-mediated stable adhesion, and extravasation.[2,3] Both P- and E-selectins are expressed in activated ECs.[4] Once E-selectins are transcriptionally induced in ECs in response to inflammatory cytokines, such as interleukin-1β (IL-1β), tumor necrosis factor-α (TNF-α),[5] and lipopolysaccharide (LPS),[6] they bind different glycosylated ligands in leukocytes, including P-selectin glycoprotein ligand-1 (PSGL-1), CD44, and E-selectin ligand-1 (ESL-1).[7,8] P-selectin is a transmembrane protein residing across the membranes of platelet granules and endothelial Weibel–Palade bodies within ECs. In response to inflammation and thrombogenic challenge, P-selectin rapidly translocates to the plasma membrane, serving as a cell adhesion receptor, and contributes to the weak adhesion between both leukocytes and activated platelets or ECs.[2]

Functionally, as an adhesion molecule, E-selectins are mainly engaged in promoting leukocyte adhesion and extravasation.[9] For example, E-selectin can induce β_2-integrin activation through the Syk signaling pathway and promote the transmigration of polymorphonuclear neutrophils (PMNs).[10] In mice, the lack of E-selectin retains the number of rolling leukocytes but reduces their stable arrest on cytokine-activated microvascular endothelium.[8]

Leukocyte extravasation is a complex multistep cascade that requires not only the activation of various adhesion molecules but also the remodeling of the actin networks in both leukocytes and ECs. Most leukocytes extravasate from circulation through the paracellular route by opening endothelial junctions at sites of inflammation.[11–13] In this process, ECs actively interact with migrating leukocytes in a complex cross-signaling network to support TEM of leukocytes.[14,15] Such cross-signaling leads to actin remodeling and changes in junctional integrity.[11] The endothelium junctions exhibit high plasticity and quickly respond to certain stimuli, such as fluid shear stress and inflammatory mediators.[11,16] Maintenance of vascular barrier function depends on the integrity and stability of endothelial adherence junctions (AJs) mediated by vascular endothelial cadherin (VE-cadherin).[17] Phosphorylation of Tyr residues of VE-cadherin differentially regulates vascular permeability and the capacity of leukocytes to transmigrate across the endothelium.[18]

In addition to supporting the physical linkage of leukocytes to the luminal surface of the endothelium, selectins play a role in signal transduction during leukocyte–endothelial interactions. Leukocyte adhesion induces E-selectin clustering on ECs, which is partially dependent on Rho GTPase activity.[19] Binding of E-selectin and its ligands activates signaling *via* MAPK, ERK/Src, or MLC/p38 pathways in ECs.[20,21] Leukocyte adhesion to cytokine-activated human umbilical vein ECs (HUVECs), or antibody-induced cross-linking of EC surface E-selectins, results in the transmembrane linkage of E-selectin to the endothelial cytoskeleton via its cytoplasmic domain.[22] While it is both known that E-selectin connects to F-actin through actin binding proteins,[22] and the actin cytoskeleton regulates the junctional integrity separately,[11,16] there is still no direct evidence on how E-selectins regulate the endothelial junction integrity to influence leukocyte extravasation.

Therefore, we examined how E-selectin-induced actin remodeling in ECs contributes to PMN transmigration through E-selectin perturbations. Accordingly, the TEM dynamics of PMNs were analyzed in a time-dependent manner. Furthermore, the correlation of endothelial integrity with the engaged actin-related protein 2/3 (Arp2/3) complex and cortactin has been discussed.

2 | MATERIALS AND METHODS

2.1 | Reagents

PE-labeled antihuman CD62E (336008) antibodies (Abs), isotype-matched irrelevant LEAF purified mouse IgG1 (400101), and purified rat IgG2a (400502) were obtained from BioLegend (San Diego, CA, USA). Mouse anti-human E-selectin (S9555) and anti-human Arp3 (A5979) monoclonal Abs, thymidine, heparin sodium, LPS, CK666, CK689, and DMSO were purchased from Sigma-Aldrich (St. Louis, MO, USA). Rabbit anti-cortactin phospho-specific [Tyr421] (44-854G) and [Tyr466] (PA5-38130) Abs were obtained from ThermoFisher Scientific (Waltham, MA, USA). Rabbit anti-VE-Cadherin (ab33168), anti-cortactin (ab81208), and anti-Arp2 (ab47654) Abs were purchased from Abcam (Cambridge, MA, USA). Medium 199, DMEM, trypsin, 4-(2-hydroxyethyl)-1-piperazine ethanesulfonic acid (HEPES), and Dulbecco's phosphate-buffered saline (DPBS) were purchased from GE Healthcare Life Sciences (Logan, UT, USA). Amphotericin B was purchased from Amresco (Solon, OH, USA). Basic fibroblast growth factor (bFGF), rabbit anti-VE-cadherin phospho-specific [Tyr731] (NBP2-54766), and anti-human E-selectin (NBP1-45545) Abs were obtained from R&D Systems (Minneapolis, MN, USA). Fetal bovine serum (FBS), MEM nonessential amino acids (MEM NEAA), and sodium pyruvate were obtained from

Gibco (Grand Island, NY, USA). RIPA buffer (9806), PMSF (8553), protease inhibitor (5871), and rabbit anti-human β-actin (12620) Abs were obtained from CST (Danvers, MA, USA).

2.2 | Neutrophil isolation and preparation

Whole human blood was obtained from healthy, unmedicated donors, after informed consent, as approved by the Animal and Medicine Ethical Committee of the Institute of Mechanics, Chinese Academy of Sciences. Donors were randomized irrespective of sex and age. Briefly, PMNs were isolated from blood samples using the density gradient media Histopaque-1119 and Histopaque-1077 (Sigma-Aldrich, St. Louis, MO, USA), as described previously.[10] Isolated PMNs were suspended in ice-cold DPBS and kept on ice until use. Collected cells were used within 3 hours of isolation, and cell density was determined using a hand-held cell counter (Scepter 2.0, Millipore, Germany).

2.3 | Cells culture and isolation

HUVECs (ATCC, Manassas, VA, USA) were cultured routinely as previously described.[10] Cells from passage 4 were plated on collagen-I-coated 35 mm glass-bottomed culture dishes (D35-14-0-N, Cellvis, Mountain View, CA, USA) to form a monolayer and then treated with 1 μg/ml LPS for 4 hours prior to cell transmigration tests. In some cases, HUVECs were pretreated with either 200 μM CK666 or CK689 inhibitor, for 15 minutes and then washed with DPBS, before adding PMNs. The inhibitors, CK666 and CK689, were dissolved in DMSO, with the pure DMSO serving as control. Human embryonic kidney (HEK)-293FT cells (ATCC, Manassas, VA, USA) were cultured in DMEM supplemented with 10% FBS, 1% NEAA, and 1 mM sodium pyruvate.

2.4 | shRNA transfection of E-selectin in HUVECs

A short hairpin RNA (shRNA) plasmid (ID: TRCN0000057790), delivered with a commercial lentiviral system (Sigma-Aldrich, St. Louis, MO, USA), was used for E-selectin knockdown in HUVECs. The scrambled and packaging plasmids were kindly provided by Dr. J. Luo, Peking University, Beijing, China. HEK-293FT cells were used for lentivirus preparation. For transfection, HEK-293FT cells were seeded at 1×10^4 cells/cm^2 in 2 mL culture medium, containing DMEM, 10% FBS, 1% NEAA, and 1 mM sodium pyruvate without penicillin and grown to 60% confluence. Opti-MEM was used to form a transfection complex containing fugenHD (Promega, Madison, WI, USA) and packaging plasmids, before dropwise addition to the cells. The suspension was then incubated for 12-16 hours and replaced with DMEM supplemented with 30% FBS for 48 hours. The virus-containing supernatants were obtained and filtered through a 0.45 μm filter. For infection, 500 μL virus-containing supernatants, 500 μL complete medium, and polybrene (final concentration: 8 μg/mL) were added. HUVECs at passage 4 were then incubated in the virus-containing medium for 48 hours.

2.5 | Real-time PCR analysis

Total RNA was isolated from HUVECs using a commercial RNA extraction kit (Tiangen, Beijing, China) according to the manufacturer's instructions. The corresponding cDNA was obtained using a commercial kit, ReverTra Ace-a (Toyobo, Tokyo, Japan), with 1 μg of RNA (total volume: 20 μL per reaction). A reverse transcriptase-polymerase chain reaction was performed using a quantitative real-time amplification system (QuantStudio 7, ThermoFisher Scientific, Waltham, MA, USA) following the manufacturer's protocol. Briefly, 10 μL amplification mixture per well was amplified as follows: denaturation at 95°C for 10 seconds, annealing at 60°C for 30 seconds, and extension at 72°C for 30 seconds. The cycle time (Ct) values obtained were used to quantify the relative expression of the genes of interest. The primer sequences used for the qPCR tests of related adhesion molecules are listed in Table S1. GAPDH was used as an internal control. The fold change of the target genes in all cases was calculated and presented as relative expression values.

2.6 | Live cell imaging and transmigration assay

Cells were grouped into either intact cell lines with no transfection or infected cell lines with scramble-plasmid (*scr*) or shRNA-E-selectin knockdown (*shE-sel*) transfection. After LPS treatment, the intact and infected HUVEC monolayers were washed twice with DPBS at 37°C and replaced with fresh media or treated with CK666, CK689, or DMSO, as described above. A total of 5×10^5 isolated PMNs were added to the HUVEC monolayer and allowed 1–2 minutes to adhere before imaging. Time-lapsed differential interference contrast (DIC) imaging was captured at 30 seconds intervals for 1 hours using an IX81 automatic inverted microscope (Olympus, Tokyo, Japan) equipped with an electron-multiplying charge-coupled device camera (iXon Ultra 897, Andor, UK). The experiments were conducted in a custom-made heating device, with temperature control (37 ± 0.5°C) and 5% CO_2 supply, during live cell imaging.

PMN transmigration was identified by visualizing the brightness change from the DIC images. The ratio of PMN transmigration was calculated by dividing the number of PMNs transmigrated per 5 min, by the total number of adhered PMNs in the field-of-view, at $t = 45$ minutes.[10] At 45 minutes, nearly all the PMNs in the focal plane adhered to the HUVEC monolayer, providing a stable baseline to estimate the PMN transmigration ratio.

2.7 | AFM test

A dimension icon atomic force microscope (AFM) (Bruker, BioScope Catalyst, Billerica, MA, USA) operated in PeakForce Quantitative Nanomechanics (QNM) mode, was employed to collect the topographical and modulus images of the HUVEC monolayer as previously described.[23,24] Briefly, the QNM-Live Cell (PFQNM-LC) probes (Bruker AFM Probes, Camarillo, CA, USA) were used with a spring constant of 0.07 N/m, tip length of 17 μm, and tip radius of 65 nm. The scanning size was 100×100 μm^2 with a resolution of 256×256 pixels, and the entire surface of a HUVEC cell was scanned point-by-point to obtain the individual elastic modulus values, at an indentation depth of 400–500 nm. All experiments were performed with ≥3 independent repeats at 25°C. A HUVEC cell was divided into two regions of the cell body, and cell periphery, in the height image. Average Young's modulus is calculated as the mean of the values at each point in the region. Data were analyzed using Nanoscope Analysis Version 1.8 (Bruker, Santa Barbara, CA, USA).

2.8 | Western blotting

After 4 h of LPS treatment, infected HUVEC monolayers were incubated with PMN for 30 minutes, washed in cold DPBS, and lysed in a 10 cm plate with 400 μL buffer, containing 20 mM Tris-HCl (pH 7.5), 150 mM NaCl, 1 mM EDTA, 1 mM EGTA, 1% sodium deoxycholate, 2.5 mM sodium pyrophosphate, 1 mM β-glycerophosphate, 1 mM Na_3VO_4, 1 μg/mL leupeptin, 1% nonyl phenoxypolyethoxylethanol (NP-40) with PMSF, and protease inhibitor. Cell lysates were collected and kept on ice for 30 minutes before centrifugation at 14 000 $\times g$ for 8 minutes at 4°C. The supernatants were then collected and denatured at 95°C. Samples were separated by SDS-PAGE, transferred to PVDF membranes and incubated with primary Abs overnight. Afterwards, the membranes were incubated with secondary Abs for 1 hours at 25°C and proteins visualized using enhanced chemiluminescence (Bio-Rad, Hercules, CA, USA, 170-5060). The following primary Abs were used: anti-E-selectin (1:1000), cortactin (1:1000), anti-VE-cadherin (1:1000), anti-β-actin (1:2000), anti-GAPDH (1:2000), anti-cortactin phospho-specific [Tyr421] (1:500), anti-cortactin phospho-specific [Tyr466] (1:1000), and anti-VE-cadherin phospho-specific [Tyr731] (1:1000). For the quantification of protein phosphorylation level, fold change of the target protein is presented as relative expression values between the *scr* and *shE-sel* HUVECs with GAPDH used as the internal reference.

2.9 | Proximity ligation assay

Proximity ligation assay (PLA) was performed with the Duolink In Situ Detection Reagents Red DUO9210 (Sigma-Aldrich, St. Louis, MO, USA), according to the manufacturer's instruction. Briefly, PMNs were added to the HUVEC monolayers after 30 minutes, washed with DPBS, fixed in 4% PFA for 15 minutes at 25°C, permeabilized with 0.1% Triton X-100 (w/v) for 15 minutes, and then blocked with PBS/BSA for 60 minutes at 37°C. Primary Abs were diluted with Ab diluent and added to the samples. After overnight incubation at 4°C, two PLA probes were diluted 1:5 and incubated with samples for 60 minutrs at 37°C, followed by the ligation mix incubation for 30 minutes at 37°C, and then the amplification mix was incubated for 100 minutes at 37°C. Finally, Duolink In Situ Mounting Medium with DAPI was used to mount the samples for 15 minutes. The samples were analyzed using a confocal laser scanning microscope (LSM880, Zeiss, Oberkochen, Germany), while PLA signals were visible as fluorescent dots.

2.10 | Immunofluorescence staining and imaging

For immunostaining, intact or infected HUVEC monolayers pretreated with LPS were washed, fixed, and immunostained, as previously described.[10] The primary Abs were diluted and added to the samples, followed by incubation overnight at 4°C. Secondary Abs in blocking buffer were added and incubated for 1 hours at 37°C. The stained samples were then stored at 4°C for imaging by confocal microscopy. Collected images were analyzed using ImageJ Version 1.53c software (National Institute of Health, Bethesda, MD, USA).

Morphological analysis of cell-cell junctions was conducted for confluent HUVEC monolayers stained with VE-Cadherin. Three morphological categories were defined: straight, finger, and reticular junctions, as reported in the literature.[25] Briefly, a total of 12-15 images were collected in each case. Junctions were identified using a pre-set 20 μm^2 patch in each image, while counting the amount of times a category appears. The percentage of patches per image was estimated as the ratio of patches per category to the total number of patches, and the mean percentage was averaged for all

images in that case. This analysis was performed in a manual, blinded fashion. For actin network analysis at cell junctions, F-actin stained images were opened in ImageJ, and the plugin Fibriltool was used to obtain the value of actin anisotropy, for evaluating the organized configuration of actin fibers.[26] The estimated values ranged between 0 and 1, with 0 denoted as disordered (*isotropic*) structures and 1 to completely ordered (*anisotropic*) structures.

2.11 | Determination of the rate of lamellipodium protrusion

For living-cell staining, the HUVEC monolayers were incubated with both 0.5 μM SiR-actin (Spirochrome Kit, Cytoskeleton, Denver, CO, USA),[27] to label the F-actin, and 10 μM Verapamil to further enhance the F-actin signal, for 4 hours at 37°C. The intact or infected HUVEC monolayers were then washed twice with DPBS at 37°C and replaced with fresh media supplemented with CK666, CK689, or DMSO, as described above. Live cell imaging of fluorescent HUVECs was conducted by confocal laser scanning microscope (LSM880, Zeiss, Oberkochen, Germany) with 63× (1.35 NA) oil-immersion objective at 37°C, with 5% CO_2 for 5 minutes at 2 seconds intervals. Zen software Version 2.3 lite (Carl Zeiss, Gottingen, Germany) was used for image acquisition and analysis. Kymographs were generated using ImageJ software along the lamellipodia moving direction (Figure S1A,B). The target regions with lamellipodia appearance at each time point were pasted next to each other along the *y*-axis.[28] Protrusion rates were then determined based on the resulting kymograph in a time-lapsed series by measuring the distance of lamellipodia tips (*x*-axis) over time (*y*-axis).

2.12 | Scratch wound assay

Infected HUVEC monolayers were seeded in six-well plates till confluence and then wounded by scraping with a sterile pipette tip along the center of each monolayer. The wounded monolayers were then washed with PBS to remove the detached cells and cultured in medium containing 2% FBS for 12 hours. Images were captured using a phase-contrast microscope (Olympus, Tokyo, Japan), either immediately or 12 hours after wounding. The healing percentage was determined by calculating the ratio of the wounding distance at 0 and 12 hours using ImageJ software.

2.13 | Flow cytometry analysis

Intact or infected HUVECs were pretreated with LPS for 4 hours, detached using 0.25% trypsin and incubated with PE-anti-E-selectin or isotype-matched irrelevant Abs in DPBS buffer on ice for 45 minutes. After washing, HUVECs were resuspended in DPBS and analyzed using a FACSCalibur cytometer (BD Biosciences, NJ, USA).

2.14 | Statistical analysis

All experiments were performed in triplicate, and the data are presented as the mean ± SE. For statistical tests, Prism software Version 6.02 (GraphPad Software, CA, USA) was used. Statistical differences were assessed with unpaired two-tailed Student's *t* test between paired data or one-way ANOVA followed by Tukey's post hoc test for grouped data. Values of $P < .05$ were considered statistically significant.

3 | RESULTS

3.1 | shRNA E-selectin transfection enhanced PMN transmigration on HUVEC monolayer.

To explore the roles of E-selectins on ECs in TEM of adhered PMNs, E-selectin expression in HUVECs monolayers was knocked down via shRNA transfection. The data indicated that E-selectin mRNA levels were significantly reduced by *shE-sel* transfection compared to *scr* transfection, while the adhesion molecules, P-selectin, ICAM-1, and VCAM-1, remained unchanged (Figure 1A). E-selectin expression in HUVECs was further tested by flow cytometry, western blotting, and immunostaining (Figure 1B-D). The *shE-sel* transfection reduced E-selectin expression in HUVECs, while similar expression was observed between *intact* (4 h-LPS stimulation without infection) and *scr* cells, and the expression in all of these was higher than that seen in the negative control without LPS stimulus (Figure 1B). These observations were further confirmed by western blotting (Figure 1C) and immunostaining (Figure 1D). Here, 4 h-LPS stimulation to HUVECs was used to mimic the enhanced E-selectin expression in the inflammatory cascade.[10] The total E-selectin expression and E-selectin fluorescence intensity was decreased in *shE-sel* compared with *scr* HUVECs. Thus, these results provide an in vitro EC model to elucidate the effects of E-selectin on the regulation of TEM dynamics of PMNs.

To test the TEM dynamics, PMNs were added to an *intact* or infected HUVEC monolayer pre-treated with LPS for 4 hours. The TEM time courses of PMNs were then visualized for 60 minutes (Figure 1E). The results indicated a transient increase in PMN TEM up to 60 minutes. Furthermore, the TEM ratio on *shE-sel* HUVECs was significantly higher (~0.3 at 60 minutes) than *scr* or *intact* HUVECs (~0.2 at 60 minutes) (Figure 1E). Optical images

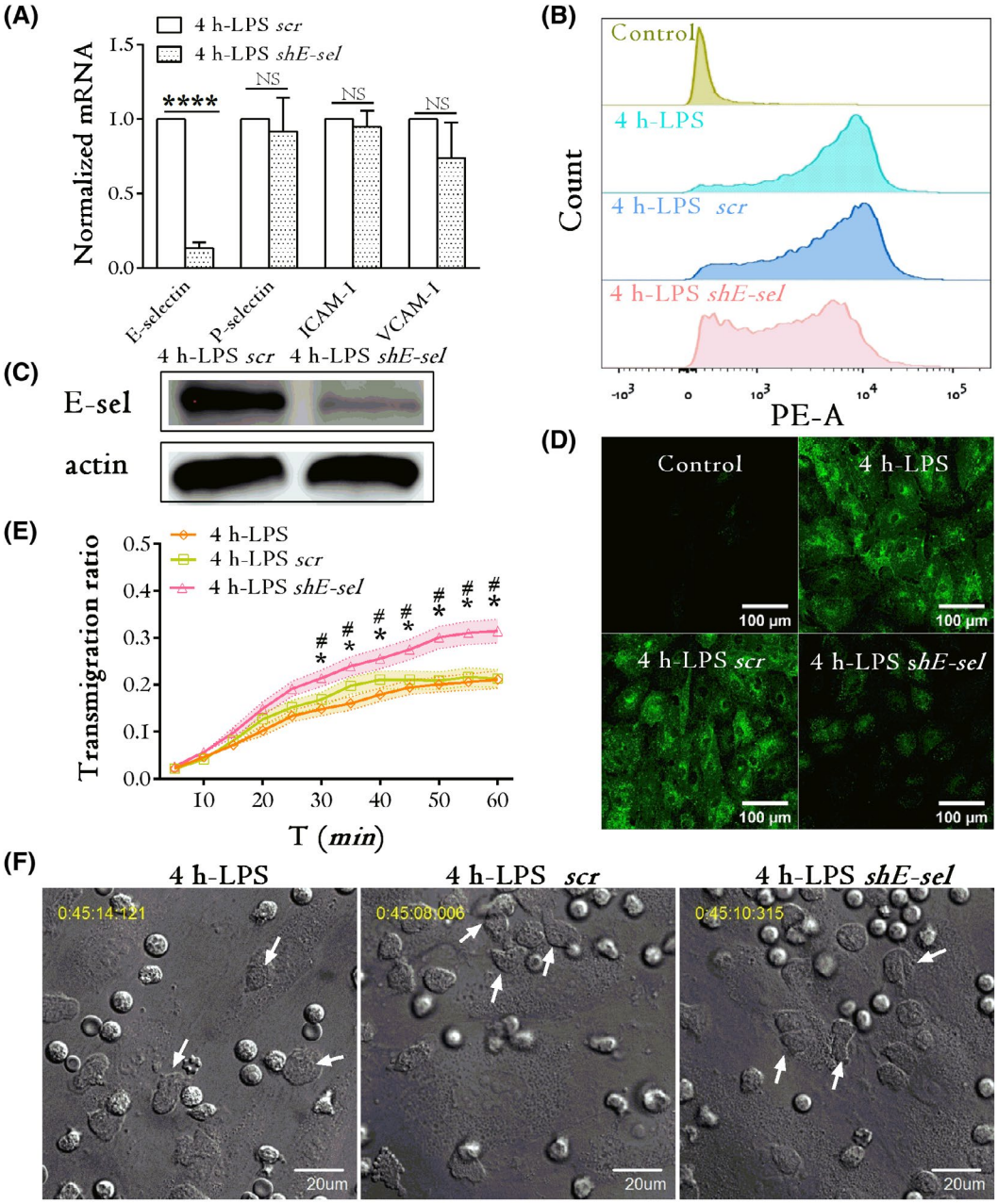

FIGURE 1 shRNA infection reduced E-selectin expression and enhanced transendothelial migration (TEM) of polymorphonuclear neutrophils (PMNs) on human umbilical vein endothelial cell (HUVEC) monolayer. A, mRNA expressions of E- and P-selectins, ICAM-1, and VCAM-1, on 4 h-LPS treated, *scr* or *shE-sel* HUVECs. Data were obtained by qPCR and normalized to the *scr* cells. E-selectin expression decreased in HUVEC monolayer examined by (B) flow cytometry analysis, (C) western blotting, and (D) immunostaining. Cells incubated with isotype-matched Abs were used as control in flow cytometry and immunostaining. E, Time courses of PMN TEM ratio on *shE-sel*, *scr*, or *intact* HUVEC monolayer. Data were obtained from at least three repeats and presented as the mean ± SE (*shadow bands*). $^{*}P < .05$, and $^{\#}P < .05$, compared with either *scr* or *intact* controls, respectively. F, Typical images of an in vitro PMN TEM assay in three cases. *White arrows* indicated the individual PMNs that are undergoing TEM

illustrated the three morphological cases of individual neutrophils undergoing TEM (*white arrows*) (Figure 1F). These data suggest that E-selectin on HUVECs negatively regulates TEM dynamics of PMNs. Moreover, these observations are not attributed to cell infection itself since no difference in TEM ratio was observed between *scr* and *intact* cells.

3.2 | E-selectin knockdown enlarged intercellular gap and reduced elastic moduli at cell-cell junction on HUVEC monolayer

We first tested the effects of E-selectin knockdown on actin remodeling. Here, F-actin staining (Figure 2A) for the *shE-sel* HUVEC monolayer showed an increase in actin filaments

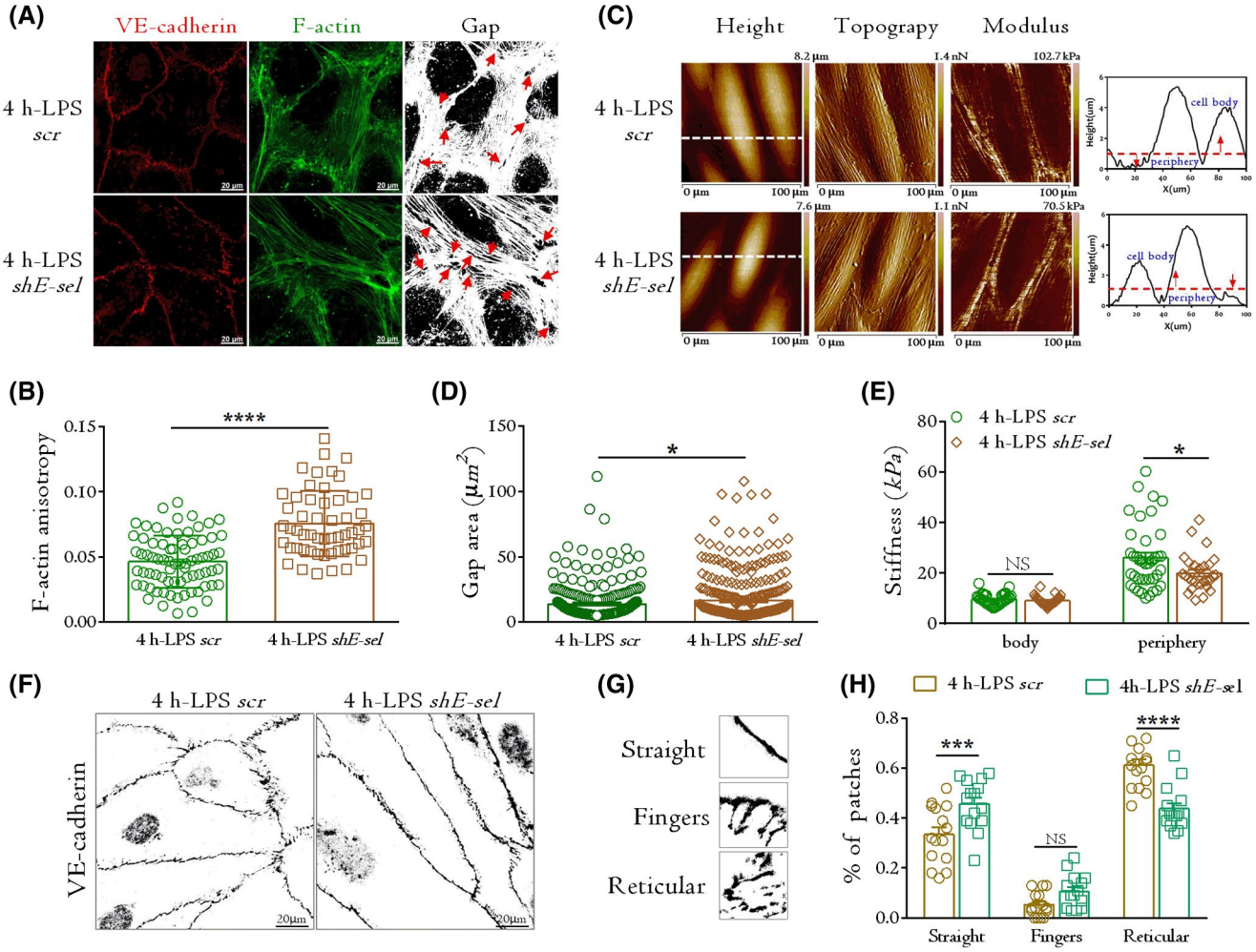

FIGURE 2 E-selectin knockdown lowered the integrity of human umbilical vein endothelial cell (HUVEC) monolayer. A, Localization of vascular endothelial (VE)-cadherin and F-actin from immunofluorescence staining. The *gap* between two neighboring cells was defined as previously reported.[51] *Red arrows* indicated the gaps at cell-cell junctions. B, F-actin anisotropy estimated for *scr* ($n = 75$) and *shE-sel* ($n = 54$) cells. For definition, see the Materials and Methods. C, Global or local elastic moduli of *scr* or *shE-sel* HUVEC monolayer. Height (*first column*), topography (*second column*), and modulus (*third column*) images of *scr* or *shE-sel* HUVEC monolayer were obtained using PFQNM-LC probes in QNM mode. Individual cell was segregated into two regions by plotting an arbitrary line in the height image (*white lines* in *first column*) and defining the cell body as the region with height ≥1 μm and the cell periphery as the one with height <1 μm (*red lines* in *fourth* column). Each panel is 100×100 μm^2. D, Quantification of inter-endothelial gap areas for *scr* ($n = 318$) or *shE-sel* ($n = 389$) gaps from 90 to 100 interconnected cells. E, Regional elastic moduli of cell body and cell periphery. Data were collected from a total of 36–46 randomly selected regions of the acquired images (see the Materials and Methods) and presented as the mean ± SE. F, Typical vascular endothelial (VE)-cadherin staining for *scr* and *shE-sel* HUVEC monolayers. G, Representative patches used for manual classification of adherence junctions in three categories: straight, fingers, and reticular junctions. H, Morphological analysis of VE-cadherin-labeled patches on *scr* ($n = 441$) or *shE-sel* ($n = 428$) cells. Data in (*B*), (*D*), (*E*), and (*H*) were presented as the mean ± SE from at least three repeats and compared using a *t* test. $^{*}P < .05$, $^{***}P < .001$, $^{****}P < .0001$

and stress fibers (actin bundles) along the junction, and a decrease in branched actin networks with high F-actin anisotropy (Figure 2B), compared to *scr* HUVECs with disorderly F-actin structures (Figure 2A), and low F-actin anisotropy (Figure 2B), implying that E-selectin knockdown induced actin remodeling.

Second, to characterize the E-selectin-induced inter-endothelial junction integrity, the size of the intercellular gap on the *shE-sel* or *scr* HUVEC monolayer was further estimated—since gap formation and closure are regulated by cytoskeletal dynamics.[29] The gaps on *shE-sel* or *scr* HUVEC monolayers can clearly be seen in Figure 2A. The average gap area on *shE-sel* HUVECs (16.5 ± 0.8 μm^2) was significantly higher than *scr* HUVECs (13.8 ± 0.7 μm^2) (Figure 2D), indicating increased loss of junctional integrity. VE-cadherin staining in *shE-sel* HUVECs further revealed morphological changes in junctional integrity (Figure 2A,F). To elaborate on the differences in junctional morphology, three categories of straight, finger, and reticular junctions were defined from the literature (Figure

2F,G).[25] Analyses indicated that E-selectin knockdown led to an increase in straight junctions and a decrease in reticular junctions in *shE-sel* HUVECs compared to those in *scr* HUVECs (Figure 2H). Since straight junctions are associated with actin filaments and stress fibers,[16] reticular junctions correspond to actin branching and junction-associated intermittent lamellipodia (JAIL) formation,[16,25,30] and the fingers are polarized structures to direct collective cell migration[31]; these observations infer E-selectin as essential for actin branching. In fact, actin branching defects induced by E-selectin knockdown increased the actin bundle and decreased the reticular junction formation in *shE-sel* HUVECs, resulting in an increased loss of junctional integrity.

Moreover, actin remodeling and junctional integrity of ECs govern the mechanical features of the entire endothelium, while leukocytes probe the underlying endothelium by extending invadosome-like protrusions into its surface.[32] We thus quantitated the effects of E-selectin knockdown on the biomechanical properties of cell–cell junctions. A QNM mode of AFM was used to simultaneously examine the height, topography and elastic modulus of the live HUVEC monolayer (Figure 2C). Here, the profiles of HUVEC height and topography were used to segregate the main body and the peripheral region of a single cell. The measured elastic moduli revealed significant differences in the cell periphery of *shE-sel* and *scr* HUVECs, with a dramatic decrease in elastic moduli at the periphery of *shE-sel* cells (Figure 2E). Taken together, these results indicated that E-selectin knockdown could enlarge the intercellular gap and reduce the peripheral moduli of the HUVEC monolayer.

3.3 | E-selectin-induced TEM of PMNs attributed to Arp2/3 complex-mediated lamellipodia protrusion and junction formation

Arp 2/3 is a key regulator in rapid actin branching, contributing to the formation and protrusion of lamellipodia,[33,34] and driving the actin assembly to promote JAIL formation and gap repair between cells.[16,35] Thus, it is hypothesized that E-selectin is also involved in Arp 2/3-mediated intercellular remodeling, which in turn regulates the TEM of PMNs. Similar time courses of transient TEM of PMNs were found in all six cases of infected HUVECs in the presence or absence of Arp 2/3 inhibition (Figure 3A,B). Interestingly, treating *scr* HUVECs with the Arp 2/3-specific inhibitor, CK666, increased the TEM compared with the addition of the inactive analog, CK689, and vehicle control DMSO (Figure 3A). In contrast, adding CK666 to *shE-sel* HUVECs had no effect on the TEM (Figure 3B), possibly due to the weakened linkage of E-selectin-Arp2/3 in *shE-sel* cells. Alternatively, Arp2/3-mediated actin branching is necessary for retaining the mechanical properties of the endothelium. AFM was also used to measure the elastic moduli of *intact* HUVECs after Arp 2/3 inhibition (Figure 3C,D). Again, adding CK666 dramatically decreased the elasticity of the entire HUVEC monolayer, especially at the periphery (Figure 3D), even with similar cell height and topography (Figure 3C), indicating that Arp2/3-mediated actin branching is required to provide mechanical support to the endothelium.

Actin remodeling also governs endothelial junctional integrity. Compared to cells treated with the inactive analogues, CK689 and DMSO, F-actin in CK666-treated HUVECs showed increased actin bundles (Figure 3E), F-actin anisotropy (Figure 3F), and decreased branched network (Figure 3E). Quantitative analysis also indicated that the gap area was dramatically increased by CK666 treatment (18.2 ± 0.8 μm^2) compared to the inactive analogues, CK689 and DMSO (14.5 ± 0.5 μm^2 and 14.4 ± 0.5 μm^2, respectively) (Figure 3G), consistent with the enlarged gaps by CK666 treatment (Figure 3E). VE-cadherin staining further revealed that CK666 treatment decreased the occurrence of reticular junctions and increased the formation of straight junctions, whereas there was no difference between CK689 and DMSO treatments (Figure 3H,I). Interestingly, CK666 treatment in *intact* HUVECs reduced the occurrence of reticular junctions (42 ± 2%) (Figure 3I) to the same level in *shE-sel* HUVECs without CK666 treatment (44 ± 2%) (Figure 2H), implying similar effects of E-selectin knockdown and actin depolymerization in the occurrence of reticular junctions.

Moreover, lamellipodia dynamics were examined to confirm the role of E-selectin and Arp2/3 in governing EC barrier integrity. Time-lapsed imaging for living-cell labeled SiR-actin indicated that E-selectin knockdown slowed lamellipodia movement compared with *the scr* group (Figure S1A). Accordingly, the rate of lamellipodia protrusion dramatically decreased after E-selectin knockdown (1.56 μm/min) compared with *scr* cells (2.89 μm/min) (Figure S1C,D,H). This decrease in lamellipodia movement may attenuate junctional recovery. Importantly, these observations on lamellipodia dynamics were consistent with the results of the wound scratch assay, showing smaller healing percentage in *shE-sel* HUVECs compared with *scr* HUVECs (Figure S2). Taken together, these findings indicated that E-selectin knockdown-induced actin remodeling significantly decreased lamellipodia movement and the ability to maintain junctional integrity (or restore the endothelial barrier), promoting PMN transmigration.

Furthermore, CK666 treatment dramatically slowed lamellipodia movement compared with CK689 and DMSO treatment (Figure S1B). Kymograph analysis indicated slower lamellipodia dynamics in the case of CK666 treatment (Figure S1E-G). In accordance with this observation, the rate of lamellipodium protrusion was significantly decreased by CK666 treatment (1.31 μm/min), compared to its inactive analog, CK689 and DMSO control (2.76 and 2.58 μm/min,

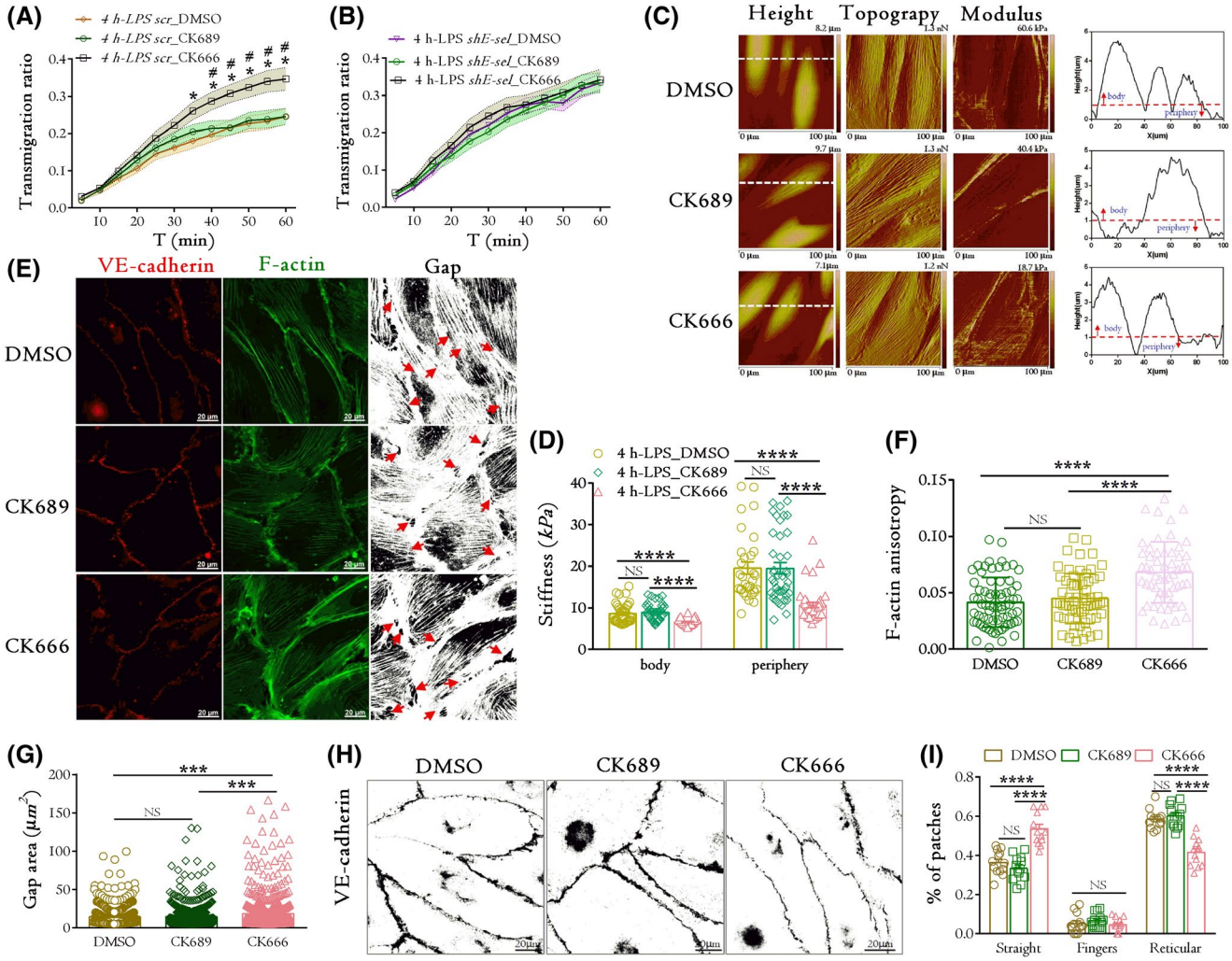

FIGURE 3 E-selectin regulated PMN transmigration via Arp2/3 complex. Effects of Arp2/3 inhibition on the transendothelial migration (TEM) of polymorphonuclear neutrophils (PMNs) across *scr* (A) or *shE-sel* (B) human umbilical vein endothelial cell (HUVEC) monolayer. Data were obtained from at least three repeats and presented as the mean ± SE (*shadow bands*). $^{\#}P < .05$ and $^{*}P < .05$, compared with CK689 and dimethyl sulfoxide (DMSO) controls, respectively. Effects of Arp2/3 inhibition (C, D) in elastic moduli of *intact* HUVECs at cell–cell junction. Data were collected from a total of 31-43 randomly selected regions of the acquired images (see the Materials and Methods) and presented as the mean ± SE in D. (E, F, G) F-actin distribution and junctional gap presence in Arp2/3-inhibited HUVEC monolayer. F-actin anisotropy was estimated for DMSO ($n = 70$), CK689 ($n = 63$), and CK666 ($n = 56$) cases (*F*). *Red arrows* indicated the gaps at cell–cell junctions (E), and total 527-700 gaps of 90-100 interconnected HUVEC cells were collected (G). Regulation of Arp2/3 complex in the formation of adherence junctions (H, I). Morphological analysis of vascular endothelial (VE)-cadherin-labeled patches by CK666 ($n = 324$), CK689 ($n = 380$), and DMSO ($n = 356$) treatment (*I*). Data were obtained from at least three repeats and presented as the mean ± SE in D, F, G, and I, $^{***}P < .001$, $^{****}P < .0001$. In all the panels, CK666 is an Arp2/3-specific inhibitor, while CK689 served as inactive analogue and DMSO as vehicle control

respectively) (Figure S1I). Collectively, these results indicated negative regulation of E-selectin on TEM of PMNs, attributed to Arp2/3-mediated actin remodeling, and lamellipodia dynamics at the cell–cell junction.

3.4 | E-selectin activated Arp2/3 complex via cortactin pathway

Cortactin is a multidomain scaffold protein involved in cortical actin assembly, dynamic actin rearrangement,[36] in which its N-terminal domain binds and stabilizes the Arp2/3 complex, and F-actin.[37] Cortactin also binds to ICAM-1 and E-selectin on ECs, with subsequent phosphorylation by Src family kinases.[22] As both E-selectin and cortactin are crucial for leukocyte TEM via regulating EC cytoskeletal remodeling, we hypothesized that cortactin may be a critical linker of E-selectin integration to cytoskeletal remodeling of ECs, thereby regulating TEM of PMNs. Thus, we first tested the phosphorylated level of cortactin in infected HUVECs treated with PMNs. E-selectin knockdown lowered the cortactin phosphorylation at Tyr 466 and Tyr421

sites (Figure 4A,B), confirming the cortactin involvement in PMN transmigration. Next, PLA was used to visualize the in situ protein–protein interplay among E-selectin, cortactin, and Arp2/3. Technical specificity was first validated, where no PLA signals were detectable when an irrelevant IgG was paired with a specific antibody against E-selectin, cortactin, or Arp2/3 (Figure S3). Interestingly, PLA signals tended to accumulate at PMN adhesion sites (Figure 4C-E), indicating the interplay of multiple E-selectin-cortactin, cortactin-Arp2/3, and E-selectin-Arp2/3 pairs, around the sites. As expected, these interactions were significantly weakened by E-selectin knockdown (Figure 4F). Collectively, these data indicated that E-selectin knockdown reduces the function of Arp2/3-mediated cell–cell junction remodeling via cortactin engagement.

3.5 | Kinetic analysis of PMNs during TEM

PMN transmigration in vivo is a dynamic process, and its kinetic features are key to the underlying functions. Our in vitro data indicated that the TEM time courses of PMNs exhibited a transient increase in the TEM ratio without reaching a plateau within the 60 min observation window (Figures 1E

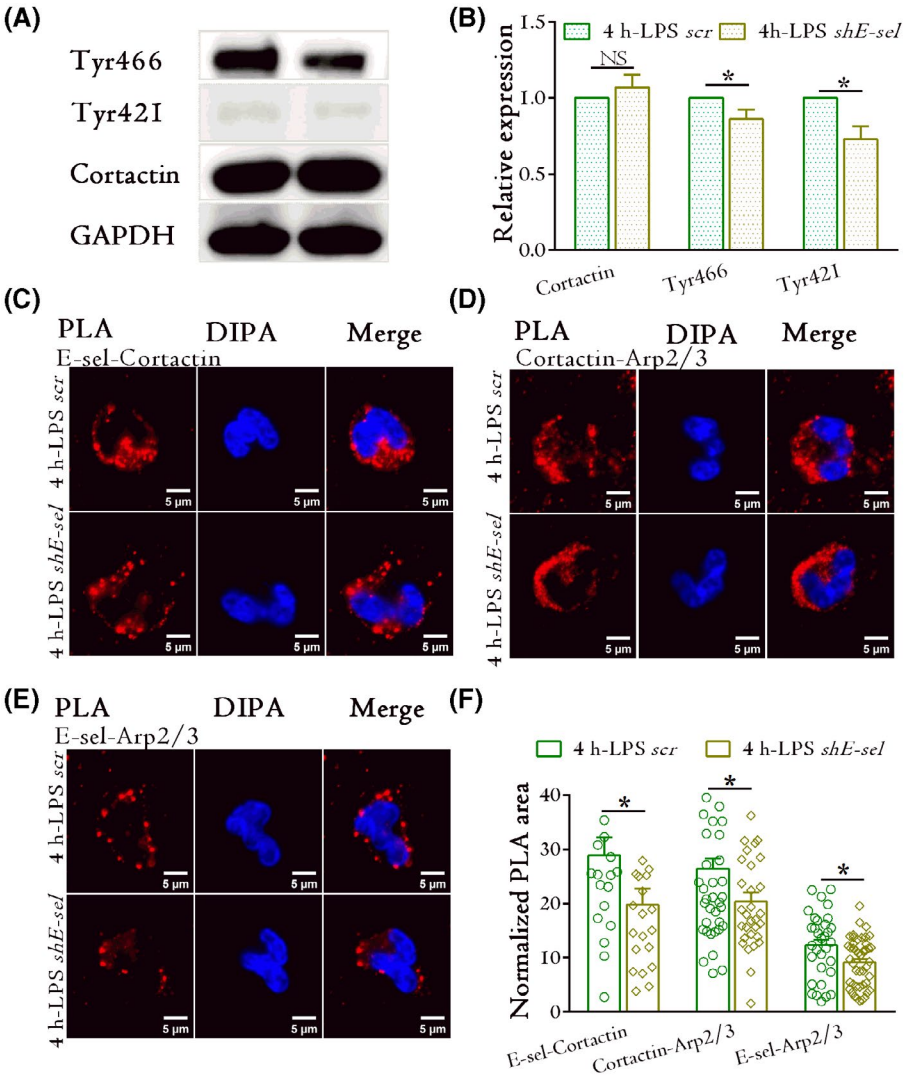

FIGURE 4 E-selectin manipulated Arp2/3 localization via associated cortactin. Immunoassay of phosphorylated Tyr466 and Tyr421 of cortactin (A) and their quantifications of the phosphorylation level (B) in 4 h LPS- and 30 minutes polymorphonuclear neutrophil (PMN)-treated *scr* or *shE-sel* human umbilical vein endothelial cell (HUVEC) monolayers. Data of at least three repeats were normalized to *intact* HUVECs and presented as the mean ± SE and compared using a *t* test. $^{*}P < .05$. Typical images of in situ proximity ligation assay (PLA) for the paired E-selectin-cortactin (C), cortactin-Arp2/3 (D), and E-selectin-Arp2/3 (E) interplay in *scr* or *shE-sel* HUVEC monolayer. Three paired primary Abs were used separately: mouse anti-E-selectin and rabbit anticortactin, rabbit anticortactin and mouse anti-Arp3, or mouse anti-E-selectin and rabbit anti-Arp2 Abs. Two anti-Arp2/3 Abs raised from different species were used due as per requirement in PLA tests. Nuclei were stained with DAPI (*blue*). Quantification of dispersed *red dots* in C–E (F). Data were collected from at least three repeats from a total of 21–41 cells and presented as the mean ± SE. $^{*}P < .05$

and 3A,B). Thus, an exponential equation was proposed to conduct further kinetics analysis:

$$y(t) = y_\infty \{1 - \exp(-t/\tau)\} \quad (1)$$

where $y(t)$ is the TEM ratio at time t, y_∞ denotes the plateau value of the TEM ratio, and τ is the characteristic time point to reach the value of $y_\infty(1-1/e)$. For each case, fitting corresponding y-t curves using Equation (1) returned the estimated (y_∞, τ) value, and averaging all the paired (y_∞, τ) values from multiple repeats yielded its mean ± SE. Fitting these parameters enabled estimation of the plateau value and the characteristic TEM time scale of PMNs, representing PMN transmigratory capacity and kinetic rate, respectively. Data sets with either TEM < 0.1 or relative coefficient $R^2 < 0.5$ were excluded (6.1%–31.6% of total data sets) for comparisons among different cases, assuring that the reliability of comparisons are maintained for the majority of data sets.

The above fitting indicated that the plateau value y_∞ was dramatically increased by E-selectin knockdown (0.52) compared to *scr* (0.41) and *intact* HUVECs (0.36) (Figure 5A). y_∞ was highly enhanced in *scr* HUVECs after treatment with the Arp2/3 inhibitor, CK666 (0.57), compared with the inactive analog CK689 (0.35), and vehicle control DMSO (0.36), however, remained indifferent among the three treatments for *shE-sel* HUVECs (Figure 5B). Accordingly, these estimations collaborated the consistency of the TEM ratio with measured values (Figures 1E and 3A,B) and predicted the plateau values of the TEM ratio.

In contrast, the estimated τ values were similar among the different cases. Specifically, τ was 48.2, 44.0, and 45.0 minutes, for *shE-sel*, *scr*, and *intact* HUVECs, respectively (Figure 5C). Treating with CK666, CK689, or DMSO, returned 49.6, 45.0, and 42.8 minutes, for *scr* HUVECs, and 45.3, 47.7, and 47.6 minutes, for *shE-sel* HUVECs, respectively (Figure 5D). These comparable τ values could be due to E-selectin knockdown or treating *scr* ECs with Arp2/3 inhibitor, inducing faster dynamics of PMN transmigration, since the time to reach the enhanced TEM capacity is similar (ie, $y(\tau) = y_\infty(1-1/e)$) in both treatments.

3.6 | P-selectin played a complementary role in mediating PMN TEM on shE-sel HUVEC monolayer

Both E- and P-selectins on HUVECs can activate β_2-integrins on PMN, thereby promoting PMN transmigration, while the two selectin–ligand pairs play complementary and competitive roles.[10,38] Thus, it is possible for P-selectins to take over the functions of activating β_2-integrins when E-selectin is knocked down to initiate PMN transmigration. To test this, we applied a blocking assay to test the engagement of P-selectins. Adding anti-P-selectin Abs G1 reduced the TEM of PMNs in *shE-sel* HUVECs (Figure 6B), while no effects were observed in *scr* HUVECs (Figure 6A), implying partial P-selectins "takeover of E-selectins" role in mediating PMN transmigration in *shE-sel* HUVECs. Moreover, no differences

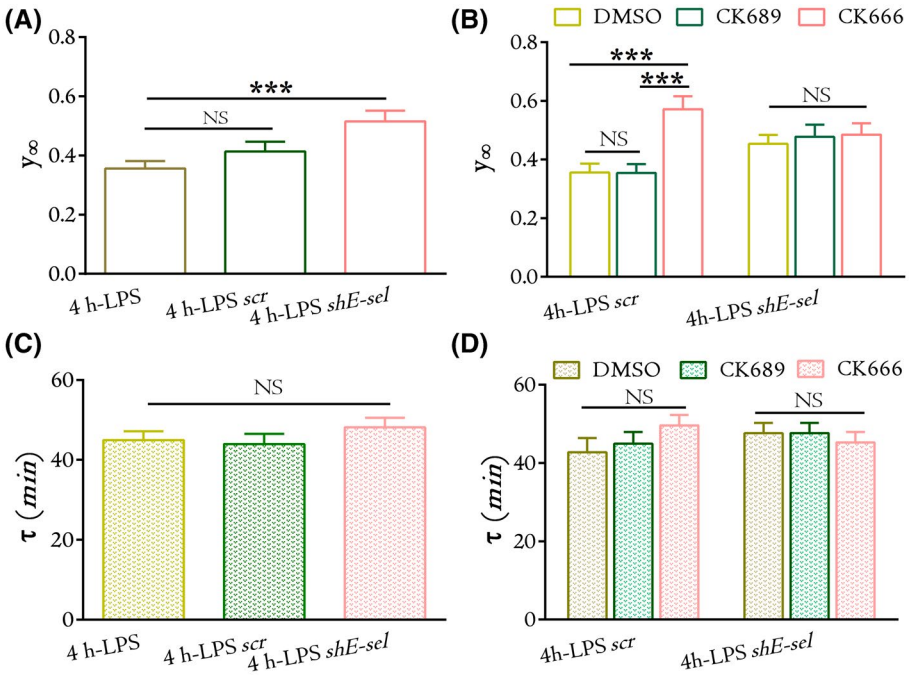

FIGURE 5 Kinetic analysis of polymorphonuclear neutrophils (PMNs) during transendothelial migration (TEM). Time courses of TEM ratio in Figures 1E and 3A,B were fitted by an exponential equation, $y(t) = y_\infty\{1 - \exp(-t/\tau)\}$. Estimated plateau value y_∞ (A,B) and characteristic time τ (C,D) from individual fitting in each case, with at least three repeats, were lumped and presented as the mean ± SE. $^{***}P < .001$

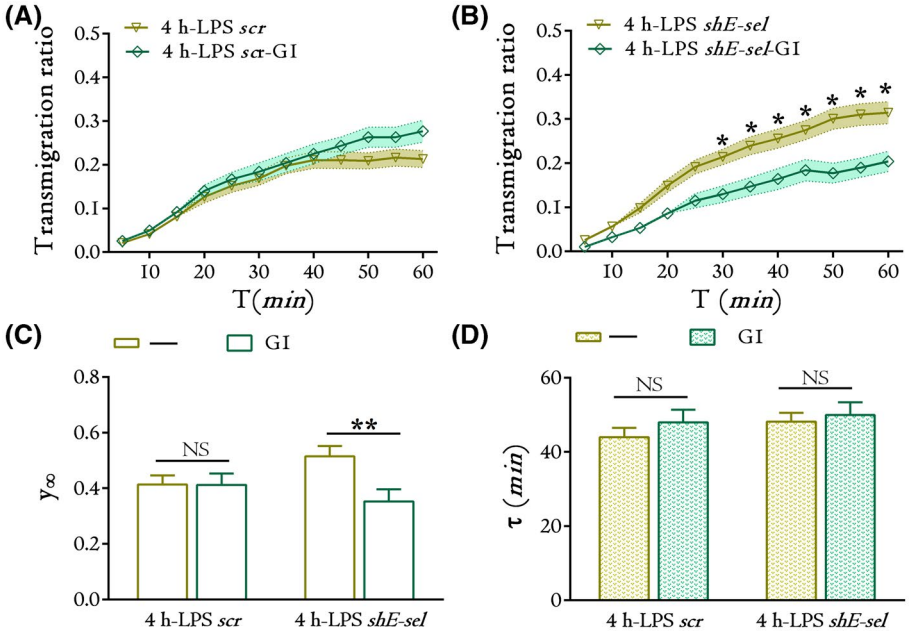

FIGURE 6 Complementary roles of P-selectin for polymorphonuclear neutrophils (PMNs) during transendothelial migration (TEM). Effects of anti-P-selectin blocking antibody G1 on the TEM of PMNs across *scr* (A) or *shE-sel* (B) human umbilical vein endothelial cell (HUVEC) monolayer. Data were obtained from at least three repeats and presented as the mean ± SE (*shadow bands*). $^{*}P < .05$. Time courses of TEM ratio in A and B were fitted by an exponential equation, $y(t) = y_\infty\{1 - \exp(-t/\tau)\}$. Estimated plateau value y_∞ (C) and characteristic time τ (D) from individual fitting in each case, from at least three repeats, were lumped and presented as the mean ± SE. $^{**}P < .01$

were found in the number of adhered PMNs on *shE-sel* and *scr* HUVECs (Figure S4), indicating a complementary role of P-selectins in mediating PMN adhesion when E-selectins were knocked down. Again, fitting Equation (1) with correlating TEM time courses indicated a dramatic decrease in the plateau value y_∞ by G1 blocking in *shE-sel* HUVECs (0.35), compared to nonblocking *shE-sel* HUVECs (0.52) while yielding comparable values for *scr* HUVECs (Figure 6C). The estimated characteristic time τ retained similar values in all cases (44.0–50.0 min) (Figure 6D). These results indicated that P-selectin overlapped the function in promoting the TEM of PMNs when E-selectin was knocked down.

4 | DISCUSSION

ECs have long been considered a passive barrier when leukocytes extravasate from the bloodstream into the underlying tissue. In fact, leukocyte TEM possesses active crosstalk between leukocytes and ECs under inflammatory conditions.[35] ECs are able to actively interact with migrating leukocytes in a complex cross-signaling network to support TEM of leukocytes.[14,15] Such cross-signaling is engaged in cellular adhesion molecules on the cell surface, and intracellular signaling molecules for actin remodeling, and junctional integrity.[11] Meanwhile, increased E-selectin expression in activated ECs is known to promote PMN extravasation, by increasing PMN adhesion and increasing EC permeability. In this study, we unexpectedly found that E-selectin knockdown upregulates TEM of PMNs with higher and faster dynamics by Arp2/3-mediated actin remodeling, and lamellipodia formation at the EC side, which in turn downregulates the adhesive function of VE-cadherin, and subsequent junctional integrity. This process is positively correlated with cortactin phosphorylation and Arp 2/3 activation, resulting in increased actin bundles, and decreased reticular junctions. We have proposed a working model to illustrate the roles of Arp2/3- and cortactin-mediated endothelial actin remodeling and junctional integrity in mediating the TEM of PMNs (Figure 7).

In contrast to existing evidence that cytokine-induced E-selectin upregulation in ECs usually promotes TEM of PMNs,[8–10,39] our novel finding shows that E-selectin knockdown on HUVECs dramatically increases transmigration of adhered PMNs (Figure 1E). This is not due to the capacity of PMN adhesion, since no differences were found in the number of adhered PMNs on *shE-sel* and *scr* HUVEC monolayers (Figure S4). Therefore, in the absence of E-selectin, active adaptation of cellular adhesion molecules occurs from the EC side (not the PMN side), to continue its function in adhesion of PMNs.[38] One example is the potential function of P-selectins on ECs, since blocking P-selectin via antibody G1 significantly decreases PMN transmigration in *shE-sel* to the same level as *scr* HUVECs (Figure 6), partially supporting the above hypothesis. Notwithstanding, E-selectin knockdown reduces Arp2/3-mediated junctional integrity via cortactin, with increased intercellular gap area, and decreased

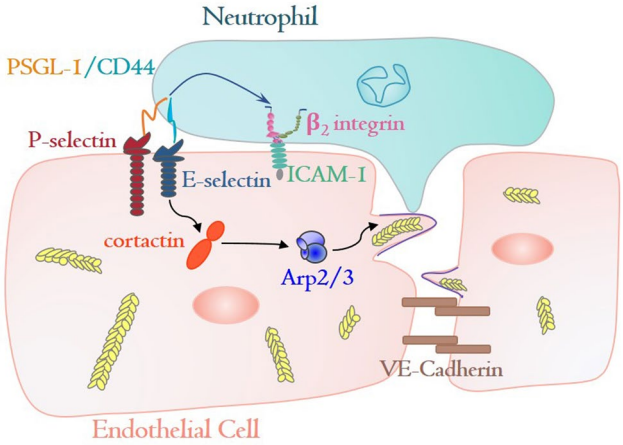

FIGURE 7 Working model of E-selectin-dependent transendothelial migration (TEM) of polymorphonuclear neutrophils (PMNs). Negative regulation of E-selectins on PMN TEM is attributed to Arp2/3- and cortactin-mediated actin remodeling and junction repair. E-selectin knockdown weakens the activation of cortactin and Arp2/3, which prevents the formations of branched actin, lamellipodia protrusion, and reticular junction between endothelial cells (ECs). Subsequently, the adhesive function of vascular endothelial (VE)-cadherin is altered, enlarging the endothelial gap, and thus expedites the PMN transmigration

reticular junction, indicating that E-selectin knockdown lowers physical barriers for TEM of PMNs. Thus, the presence of E-selectins on the surface of ECs regulates PMN transmigration in a "*double-edged sword*" manner between retaining endothelial integrity and supporting PMN adhesion. Since the former hinders, but the latter favors the TEM of PMNs, the final outcome of E-selectin engagement is governed by the competition between these two functions. The evidence from this study would strongly suggest that its roles in reducing endothelial junction integrity are dominant.

PMN extravasation is related to the phosphorylation of VE-cadherin at different sites, for example, the roles of Tyr731 dephosphorylation in the integrity of endothelial junctions.[11,18] To address this issue, western blotting was conducted to check the expression of VE-cadherin and its dephosphorylation at Tyr731. Intriguingly, E-selectin knockdown had no effect on Tyr731 phosphorylation but lowered the expression of total VE-cadherin (Figure S5). This finding seemed to be consistent with observations that local shortage of VE-cadherin initiates the formation of JAIL driven by the Arp2/3 complex, which in turn facilitates the formation of new VE-cadherin adhesion sites, to help maintain EC monolayer integrity.[16] Noting that the patterns of junctional VE-cadherin varied significantly (Figures 2F-H), these results suggest that E-selectin knockdown tends to enlarge the endothelial gap by destabilizing the junctional integrity.

The initial formation of cell junctions is mediated by actin-driven lamellipodia that brings adjacent cells together,[16,40] while the factors mediating lamellipodia formation are also able to regulate junctional integrity.[41–43] In this study, lamellipodial protrusion-related Arp2/3 and cortactin were examined to clarify their roles in E-selectin-mediated junctional remodeling. E-selectin knockdown dramatically weakens the linkage of E-selectin-cortactin and cortactin-Arp2/3 complexes, which downregulates the capability of junction formation and junction repairing between ECs, subsequently enlarging the endothelial gaps (Figures 2 and 3). In addition, there exists an interplay between traction stresses in ECs and tugging forces on endothelial junctions.[44] E-selectin knockdown enhanced the presentation of stress fibers (Figures 2A and S6), implying a high tugging force to induce large gaps between ECs and destabilize junctional integrity for monolayer permeability. These results confirm previous studies showing that tugging forces can generate gaps if the forces are too high, but the loss of tension on cell junctions can also destabilize the endothelial junctions.[44]

Actin remodeling and junctional integrity are associated with endothelial mechanics, and the spatiotemporal differences in the mechanical strength of the endothelial barrier crucially affect where leukocytes undergo diapedesis.[32] We evaluated the mechanical properties of ECs using an AFM assay. The results showed that E-selectin knockdown significantly decreased the stiffness of ECs at the intercellular junction (periphery) (Figure 2E), providing mechanical support for PMN diapedesis. F-actin is known to be one of the primary determinants of cellular stiffness in most cell types,[45,46] and leukocytes prefer diapedesis at locations with relatively lower F-actin density, or at the zones of lowest endothelial stiffness.[32,47] Therefore, the decreased stiffness of the endothelial periphery suggests that the density of F-actin could also have been decreased. Investigating the F-actin fluorescence intensity at the periphery in the conditions of pre-E-selectin and post-E-selectin knockdown showed a decreased normalized mean F-actin fluorescence intensity after E-selectin knockdown (Figure S6A,B), supporting the evidence that PMN diapedesis occurs at the least resistant mechanical position.[32,48,49] While F-actin anisotropy is proportional to cell stiffness in some studies,[50] E-selectin knockdown in this study resulted in a high anisotropy value with lowered total F-actin intensity and peripheral stiffness in *shE-sel* compared to *scr* HUVECs. Further analysis of F-actin distribution indicated that the peak values in *shE-sel* HUVECs were relatively high, while the number of peaks and valleys were much lower than those in *scr* HUVECs (Figures S6A and 2A), consistent with the decreased F-actin intensity and peripheral stiffness.

In conclusion, we found, for the first time, that E-selectin knockdown in ECs enhances TEM of neutrophils, by altering endothelial integrity. E-selectin knockdown destabilized the mechanical properties of ECs and its endothelial junctions, by downregulating cortactin, Arp2/3, and VE-cadherin, which in turn enhances PMN TEM via actin remodeling, lamellipodia projection, and improved junctional integrity.

Our results provide in vitro insight into the mechanisms of neutrophil transmigration from an inflammation-activated EC perspective.

ACKNOWLEDGMENTS

This work was supported by the National Natural Science Foundation of China Grants 31627804, 91642203, 11772345, and 91539119; the National Key Research and Development Program of China grant 2016YFA0501601; the Chinese Academy of Sciences Strategic Priority Research Program XDB22040101; and the Frontier Science Key Project QYZDJ-SSW-JSC018.

CONFLICT OF INTERESTS

The authors declare no competing financial interests.

AUTHOR CONTRIBUTIONS

M. Long and Y. Zhang developed the concept, designed the study, and wrote the paper; D. Huang and Q. Ding performed experiments; and M. Long, Y. Zhang, D. Huang, S. Chen, and S. Lü analyzed the data.

REFERENCES

1. Van Buul JD, Hordijk PL. Endothelial adapter proteins in leukocyte transmigration. *Thromb Haemostasis*. 2009;101:649-655.
2. McEver RP. Selectins: lectins that initiate cell adhesion under flow. *Curr Opin Immunol*. 2002;14:581-586.
3. McEver RP. Selectins. *Curr Opin Immunol*. 1994;6:75-84.
4. McEver RP, Zhu C. Rolling cell adhesion. In: Schekman R, Goldstein L, Lehmann R, eds. *Annual Review of Cell and Developmental Biology*. Palo Alto, USA: Annual Reviews; 2010:363-396.
5. Kelly M, Hwang JM, Kubes P. Modulating leukocyte recruitment in inflammation. *J Allergy Clin Immunol*. 2007;120:3-10.
6. Lorenzon P, Vecile E, Nardon E, et al. Endothelial cell E- and P-selectin and vascular cell adhesion molecule-1 function as signaling receptors. *J Cell Biol*. 1998;142:1381-1391.
7. Bevilacqua MP, Nelson RM, Mannori G, Cecconi O. Endothelial-leukocyte adhesion molecules in human disease. *Annu Rev Med*. 1994;45:361-378.
8. Milstone DS, Fukumura D, Padgett RC, et al. Mice lacking E-selectin show normal numbers of rolling leukocytes but reduced leukocyte stable arrest on cytokine-activated microvascular endothelium. *Microcirculation*. 1998;5:153-171.
9. Setiadi H, McEver RP. Clustering endothelial E-selectin in clathrin-coated pits and lipid rafts enhances leukocyte adhesion under flow. *Blood*. 2008;111:1989-1998.
10. Gong Y, Zhang Y, Feng S, Liu X, Lü S, Long M. Dynamic contributions of P- and E-selectins to beta2-integrin-induced neutrophil transmigration. *FASEB J*. 2017;31:212-223.
11. Vestweber D. How leukocytes cross the vascular endothelium. *Nat Rev Immunol*. 2015;15:692-704.
12. Schenkel AR, Mamdouh Z, Muller WA. Locomotion of monocytes on endothelium is a critical step during extravasation. *Nat Immunol*. 2004;5:393-400.
13. Alon R, van Buul JD. Leukocyte breaching of endothelial barriers: the actin link. *Trends Immunol*. 2017;38:606-615.
14. Wittchen ES. Endothelial signaling in paracellular and transcellular leukocyte transmigration. *Front Biosci*. 2009;14:2522-2545.
15. Noushargh S, Hordijk PL, Sixt M. Breaching multiple barriers: leukocyte motility through venular walls and the interstitium. *Nat Rev Mol Cell Bio*. 2010;11:366-378.
16. Abu Taha A, Taha M, Seebach J, Schnittler H-J. ARP2/3-mediated junction-associated lamellipodia control VE-cadherin-based cell junction dynamics and maintain monolayer integrity. *Mol Biol Cell*. 2014;25:245-256.
17. Weber C, Fraemohs L, Dejana E. The role of junctional adhesion molecules in vascular inflammation. *Nat Rev Immunol*. 2007;7:467-477.
18. Wessel F, Winderlich M, Holm M, et al. Leukocyte extravasation and vascular permeability are each controlled in vivo by different tyrosine residues of VE-cadherin. *Nat Immunol*. 2014;15:223-230.
19. Wojciak-Stothard B, Williams L, Ridley AJ. Monocyte adhesion and spreading on human endothelial cells is dependent on Rho-regulated receptor clustering. *J Cell Biol*. 1999;145:1293-1307.
20. Hu Y, Kiely JM, Szente BE, Rosenzweig A, Gimbrone MA. E-selectin-dependent signaling via the mitogen-activated protein kinase pathway in vascular endothelial cells. *J Immunol*. 2000;165:2142-2148.
21. Tilghman RW, Hoover RL. The Src-cortactin pathway is required for clustering of E-selectin and ICAM-1 in endothelial cells. *FASEB J*. 2002;16:1257-1259.
22. Yoshida M, Westlin WF, Wang N, et al. Leukocyte adhesion to vascular endothelium induces E-selectin linkage to the actin cytoskeleton. *J Cell Biol*. 1996;133:445-455.
23. Xu Y, Huang D, Lü S, Zhang Y, Long M. Mechanical features of endothelium regulate cell adhesive molecule-induced calcium response in neutrophils. *APL Bioeng*. 2019;3:16104.
24. Hu J, Chen S, Huang D, Zhang Y, Lü S, Long M. Global mapping of live cell mechanical features using PeakForce QNM AFM. *Biophys Rep*. 2019;6:9-18.
25. Neto F, Klaus-Bergmann A, Ong YT, et al. YAP and TAZ regulate adherens junction dynamics and endothelial cell distribution during vascular development. *eLife*. 2018;7:e31037.
26. Boudaoud A, Burian A, Borowska-Wykret D, et al. FibrilTool, an ImageJ plug-in to quantify fibrillar structures in raw microscopy images. *Nat Protoc*. 2014;9:457-463.
27. Lukinavicius G, Reymond L, D'Este E, et al. Fluorogenic probes for live-cell imaging of the cytoskeleton. *Nat Methods*. 2014;11:731-733.
28. Dimchev G, Steffen A, Kage F, et al. Efficiency of lamellipodia protrusion is determined by the extent of cytosolic actin assembly. *Mol Biol Cell*. 2017;28:1311-1325.
29. Belvitch P, Brown ME, Brinley BN, et al. The ARP 2/3 complex mediates endothelial barrier function and recovery. *Pulm Circ*. 2017;7:200-210.
30. Schnittler H, Taha M, Schnittler MO, Abu Taha A, Lindemann N, Seebach J. Actin filament dynamics and endothelial cell junctions: the Ying and Yang between stabilization and motion. *Cell Tissue Res*. 2014;355:529-543.
31. Hayer A, Shao L, Chung M, et al. Engulfed cadherin fingers are polarized junctional structures between collectively migrating endothelial cells. *Nat Cell Biol*. 2016;18:1311-1323.
32. Martinelli R, Zeiger AS, Whitfield M, et al. Probing the biomechanical contribution of the endothelium to lymphocyte migration: diapedesis by the path of least resistance. *J Cell Sci*. 2014;127:3720-3734.

33. Pollard TD. Regulation of actin filament assembly by Arp2/3 complex and formins. *Annu Rev Bioph Biom*. 2007;36:451-477.
34. Svitkina TM, Borisy GG. Arp2/3 complex and actin depolymerizing factor/cofilin in dendritic organization and treadmilling of actin filament array in lamellipodia. *J Cell Biol*. 1999;145:1009-1026.
35. Mooren OL, Li J, Nawas J, Cooper JA. Endothelial cells use dynamic actin to facilitate lymphocyte transendothelial migration and maintain the monolayer barrier. *Mol Biol Cell*. 2014;25:4115-4129.
36. Weed SA, Parsons JT. Cortactin: coupling, membrane dynamics to cortical actin assembly. *Oncogene*. 2001;20:6418-6434.
37. Uruno T, Liu J, Li Y, Smith N, Zhan X. Sequential interaction of actin-related proteins 2 and 3 (Arp2/3) complex with neural Wiscott-Aldrich syndrome protein (N-WASP) and cortactin during branched actin filament network formation. *J Biol Chem*. 2003;278:26086-26093.
38. Mark AL, Christine FN, John MR, et al. Characterization of E-selectin-deficient mice: demonstration of overlapping function of the endothelial selectins. *Immunity*. 1994;1:709-720.
39. Brodt P, Fallavollita L, Bresalier RS, Meterissian S, Norton CR, Wolitzky BA. Liver endothelial E-selectin mediates carcinoma cell adhesion and promotes liver metastasis. *Int J Cancer*. 1997;71:612-619.
40. Nelson WJ. Regulation of cell-cell adhesion by the cadherin-catenin complex. *Biochem Soc Trans*. 2008;36:149-155.
41. Kovacs EM, Goodwin M, Ali RG, Paterson AD, Yap AS. Cadherin-directed actin assembly: E-cadherin physically associates with the Arp2/3 complex to direct actin assembly in nascent adhesive contacts. *Curr Biol*. 2002;12:379-382.
42. Kobielak A, Pasolli HA, Fuchs E. Mammalian formin-1 participates in adherens junctions and polymerization of linear actin cables. *Nat Cell Biol*. 2004;6:21-30.
43. Welch MD, Mullins RD. Cellular control of actin nucleation. *Annu Rev Cell Dev Biol*. 2002;18:247-288.
44. Liu Z, Tan JL, Cohen DM, et al. Mechanical tugging force regulates the size of cell-cell junctions. *PNAS*. 2010;107:9944-9949.
45. Pesen D, Hoh JH. Micromechanical architecture of the endothelial cell cortex. *Biophy J*. 2005;88:670-679.
46. Rotsch C, Radmacher M. Drug-induced changes of cytoskeletal structure and mechanics in fibroblasts: an atomic force microscopy study. *Biophy J*. 2000;78:520-535.
47. Isac L, Thoelking G, Schwab A, Oberleithner H, Riethmuller C. Endothelial F-actin depolymerization enables leukocyte transmigration. *Anal Bioanal Chem*. 2011;399:2351-2358.
48. Martinelli R, Kamei M, Sage PT, et al. Release of cellular tension signals self-restorative ventral lamellipodia to heal barrier microwounds. *J Cell Biol*. 2013;201:449-465.
49. Rajagopal V, Holmes WR, Lee PVS. Computational modeling of single-cell mechanics and cytoskeletal mechanobiology. *Wiley Interdiscip Rev Syst Biol Med*. 2018;10:e1407.
50. Schnoor M. Endothelial actin-binding proteins and actin dynamics in leukocyte transendothelial migration. *J Immunol*. 2015;194:3535-3541.
51. Andresen Eguiluz RC, Kaylan KB, Underhill GH, Leckband DE. Substrate stiffness and VE-cadherin mechano-transduction coordinate to regulate endothelial monolayer integrity. *Biomaterials*. 2017;140:45-57.

SUPPORTING INFORMATION

Additional Supporting Information may be found online in the Supporting Information section.

How to cite this article: Huang D, Ding Q, Chen S, Lü S, Zhang Y, Long M. E-selectin negatively regulates polymorphonuclear neutrophil transmigration through altered endothelial junction integrity. *The FASEB Journal*. 2021;35:e21521. https://doi.org/10.1096/fj.202000662RR